Bulletin of Electrical Engineering and Informatics
Vol. 14, No. 3, June 2025, pp. 1830~1845
ISSN: 2302-9285, DOI: 10.11591/eei.v14i3.8397

Breast cancer detection and classification using deep learning techniques based on ultrasound image

Abdulqader Mohammed Khalaf[1], Mohammed Abdel Razek[1], Mohamed El-Dosuky[2,3], Ahmed Sobhi[1]
[1]Department of Mathematics and Computer Science, Faculty of Science, AL-Azhar University, Cairo, Egypt
[2]Department of Computer Science, Faculty of Computers and Information, Mansoura University, Mansoura, Egypt
[3]Department of Computer Science, Arab East Colleges, Riyadh, Saudi Arabia

Article Info

Article history:

Received Feb 26, 2024
Revised Nov 9, 2024
Accepted Nov 19, 2024

Keywords:

Breast cancer classification
Breast cancer detection
Breast ultrasound image
Cancer image segmentation
Deep learning technique

ABSTRACT

Breast cancer ranks as the most prevalent form of cancer diagnosed in women. Diagnosis faces several challenges, such as changes in the size, shape, and appearance of the breast, dense breast tissue, and lumps or thickening, especially if present in only one breast. The major challenge in the deep learning (DL) diagnosis of breast cancer is its non-uniform shape, size, and position, particularly with malignant tumors. Researchers strive through computer-aided diagnosis (CAD) systems and other methods to assist in detecting and classifying tumor types. This work proposes a DL system for analyzing medical images that improves the accuracy of breast cancer detection and classification from ultrasound (US) images. It reaches an accuracy of 99.29%, exceeding previous work. First, image processing is applied to enhance the quality of input images. Second, image segmentation is performed using the U-Net architecture. Third, many features are extracted using Mobilenet. Finally, classification is performed using visual geometry group 16 (VGG16). The accuracy of detection and classification using the proposed system was evaluated.

Corresponding Author:

Abdulqader Mohammed Khalaf
Department of Mathematics and Computer Science, Faculty of Science, Al-Azhar University
Nasr City, Cairo 11884, Egypt
Email: mabdulqader135@gmail.com

1. INTRODUCTION

Breast cancer is a common type of cancer that forms in the breast cells and is more common in women than in men [1]. Age, gender, family history, and genetic factors contribute to the risk. mutations, hormonal factors, personal history, and lifestyle factors [2]. Symptoms include a lump or mass in the breast, breast pain, swelling, skin irritation, nipple retraction, and redness [3]. Diagnosis and treatment involve breast examination, imaging tests, and biopsy [4]. Available treatment options encompass surgery, radiation therapy, chemotherapy, hormone therapy, and targeted therapy [5]. Prevention and awareness of breast cancer include regular self-exams, clinical breast exams, mammography screening, and a healthy lifestyle [6]. Early detection of breast cancer is essential for effective treatment, better outcomes, decreased patient suffering and financial burden, and the potential to detect the disease at an earlier stage, leading to enhanced chances of survival and recovery, as well as enabling more straightforward and cost-efficient treatment.

Breast cancer diagnosis faces several challenges, including false positives and false negatives, dense breast tissue, subjective interpretation, limited access to screening, over diagnosis and overtreatment, lack of standardized guidelines, invasive diagnostic procedures, and irregularity boundaries of tumor especially malignant tumors [7]. The problems addressed by this paper can be stated as follows: i) breast tumors do not have a fixed size or location, especially malignant tumors; ii) change in shape and difficulty get masking the tumor or identifying only the tumor area, especially malignant tumors, while benign tumors have a regular or semi-regular shape; iii) some nodules or clusters that could be interpreted as tumors, but in reality, they are not; and iv) in some cases, there are more than one tumor mass in the same area, in this case, a mask must be taken for each tumor mass separately.

Deep learning (DL), which is a subset of machine learning, has shown promise in breast cancer diagnosis and treatment, these algorithms can analyze mammograms, ultrasound (US) images, and magnetic resonance imaging (MRI) scans to detect and classify breast lesions, improve image interpretation accuracy, and predict individual risk of developing breast cancer [8]. Table 1 shows the previous work on breast cancer diagnosis based on US images along with the year of publication.

Table 1. Previous work

References	Description of the method	Year
[9]	Automatic identification using supervised block-based region segmentation and feature combination migration as the foundation	2019
[10]	Learn from noisy US images	2020
[11]	Learning from a combination of convolutional neural networks (CNN)	2020
[12]	Semi-supervised DL focused on breast imaging reporting and data system (BI-RADS) features	2020
[13]	Segmentation US with selective kernel U-Net CNN	2020
[14]	Using variant-enhanced DL for US image segmentation.	2021
[15]	Semi-supervised generative adversarial networks (GAN)	2021
[16]	Image decomposition and fusion	2021
[17]	Transfer learning with deep representations scaling	2021
[18]	Transfer learning in breast cancer diagnoses	2021
[19]	Coarse-to-fine fusion CNN for breast image segmentation	2021
[20]	Breast ultrasound (BUS) detection via vision transformers (ViT)	2022
[21]	Benchmark BUS image segmentation	2022
[22]	Automated lesion BI-RADS classification using the pyramid triple deep feature generator technique	2022
[23]	Malignant BUS images using ViT-patch	2023

Contributions can be outlined as follows: i) this paper proposed a DL model that increased the accuracy of detection and classification of breast cancer from US images; ii) the proposed model outperformed previous work, reaching 99.29% accuracy; iii) many features have been extracted to rely in detecting and classifying the type of tumor in a high and efficient manner; and iv) the proposed system was trained on masks for the tumor area and was tested on images of tumors, so the system predicted masks for these images, and the system also made masks for images of tumors that were not trained either on images or on masks. The system was also trained and tested to recognize and distinguish images and determine the type of tumor in which either benign, malignant or there is no tumor.

The subsequent sections of this paper are organized as follows: section 2 provides an overview of the previous work in breast cancer diagnosis. Section 3 provides the method. Section 4 shows the results and discussion. Finally, section 5 provides conclusion of the paper before listing some future directions.

2. PREVIOUS WORK

Liao *et al*. [9], employed the combination of DL technology with US imaging diagnosis. The tumor regions were segmented from the BUS images using a supervised block-based region segmentation algorithm. The best diagnostic outcome was achieved by establishing a combination feature model based on the depth feature of ultrasonic imaging and strain elastography. Cao *et al*. [10], proposed to tackle the issue of noisy labels during the training of breast tumor classification models, a successful technique known as the noise filter network (NF-Net) was introduced.

Moon *et al*. [11] proposed a computer-aided diagnosis (CAD) system was developed for tumor diagnosis. This system utilized an image fusion method that combined various image content representations and employed ensemble techniques with different CNN architectures on US images. Zhang *et al*. [12], proposed a new DL model semi-supervised deep learning (SSDL). This integration aimed to achieve precise diagnosis of ultrasound images, particularly when working with limited training data.

Research by Byra *et al*. [13], DL technique has been created for segmenting breast masses in US images, aiming to overcome the difficulty of automated segmentation caused by differences in breast mass size and image features. This approach employs a selective kernel (SK) U-Net CNN to modify receptive fields and combine feature maps obtained from dilated and regular convolutions. The model has demonstrated a notable relationship between the utilization of dilated convolutions and the size of breast masses in the network's expansion phase.

Ilesanmi *et al*. [14] proposed that BUS images underwent resizing and were then enhanced using the contrast limited adaptive histogram equalization method. The pre-processed image was encoded using the variant enhanced block. Ultimately, the segmentation mask was generated through concatenated convolutions. Pang *et al*. [15] proposed a semi-supervised GAN model was created to enhance BUS images. The generated images were then employed for breast mass classification using a CNN. The performance of the model was assessed using a 5-fold cross-validation approach.

Zhuang *et al*. [16] proposed the method that applies fuzzy enhancement and bilateral filtering algorithms for the enhancement of original images, obtaining decomposed images representing breast tumor clinical characteristics, fuse them through red, green, and blue (RGB) channels, choose the optimal DL feature model, and train a network for classification that utilizes adaptive spatial feature fusion technology. While Byra [17] proposed a DL-based method for classifying breast masses in US images. The approach incorporates deep representation scaling (DRS) layers between pre-trained CNN blocks. By reducing the number of trainable parameters, this technique outperforms conventional transfer learning methods and achieves improved performance.

Ayana *et al*. [18] proposed introduces transfer learning methods for the classification and detection of breast images in US. The focus is on transfer learning approaches, pre-processing techniques, pre-training models, and CNN models. Wang *et al*. [19] proposed a novel CNN with a coarse-to-fine feature fusion approach is suggested for breast image segmentation. The network comprises an encoder path, decoder path, and core fusion stream path, which collectively produce comprehensive feature representations for precise segmentation of breast lesions. Additionally, the network integrates super-pixel images and a weighted-balanced loss function to handle variations in lesion region sizes.

Ayana and Choe [20] proposed a BUViTNet which is a method for BUS detection using ViTs instead of CNNs. The approach leverages datasets containing images from both ImageNet and cancer cells to classify BUS images. The performance of the algorithm surpassed that of ViT trained from scratch, ViT-based conventional transfer learning, and transfer learning based on CNN. While Zhang *et al.* [21] presented a standard for BUS image segmentation evaluation, proposes standardized procedures for accurate annotations, and introduces a losses-based approach to assess the impact of user interactions on the sensitivity of semi-automatic segmentation.

Kaplan *et al*. [22] proposed a BI-RADS a classifier model for categorizing US breast lesions using a novel multi-class US image, utilizing bilinear interpolation and neighborhood component analysis to generate informative features for automated classification. Recently, Feng *et al*. [23] introduced an enhanced ViT architecture that incorporates a shared MLP head to the output of each patch token. This modification ensures balanced feature learning between class and patch tokens. Additionally, the model utilizes the output of the class token to distinguish between malignant and benign images. Furthermore, the output of each patch token is employed to determine if the patch overlaps with the tumor area.

3. METHOD

This system utilizes four models: preprocessing, a segmentation model, a feature evaluation stage to extract various features from the cancer mask (contour), and cancer classification model. In the first stage of the proposed system, its pre-processing the images to get rid of noise and improve them by applying the appropriate filter to them, then re-sizing and standardizing the size of all the images to be one size and format to deal with them accurately. In the second phase, were segmented the images using the U-Net method, which is one of the DL methods and techniques and is effective in dealing with medical images, especially tumors. Image segmentation is an important stage, as we obtain from it the parts that contain the tumor in order to facilitate dealing with them and isolate the tumor area to extract characteristics from it. The segmentation model uses the U-Net architecture and was trained to achieve 98.68% accuracy for training phase, and 99.29 accuracy for testing phase. After training, the actual and predicted masks were visualized for comparison. In the third stage, were features extracted from the images using the Mobilenet method, which is a DL method that is accurate and efficient and reduces the number of parameters compared to other networks, resulting in deep and lightweight neural networks. These features were relied upon to determine the type of tumor whether it is malignant, benign or not cancer (normal). Many of these characteristics were extracted to identify the tumor accurately and efficiently, and they were taken from the mask that was made on the image, as it works to isolate the tumor area in order to take characteristics from it and know the tumor's sleep through those characteristics. In the last stage came the classification phase, where one of the DL techniques, namely visual geometry group 16 (VGG16), was used to know the type of tumor and identify it based on the features that were extracted from the mask in the third stage, where after extracting the features from the mask, they are entered into the deep network to train it with the network's layers and stages, and then the identify and determined the type of tumor. The classifier model was used to classify types of breast cancer, and the resulting classifications were visualized, using a Kaggle notebook instead of Google Colab because it has better graphics processing units (GPUs), Figure 1 shows the proposed architecture.

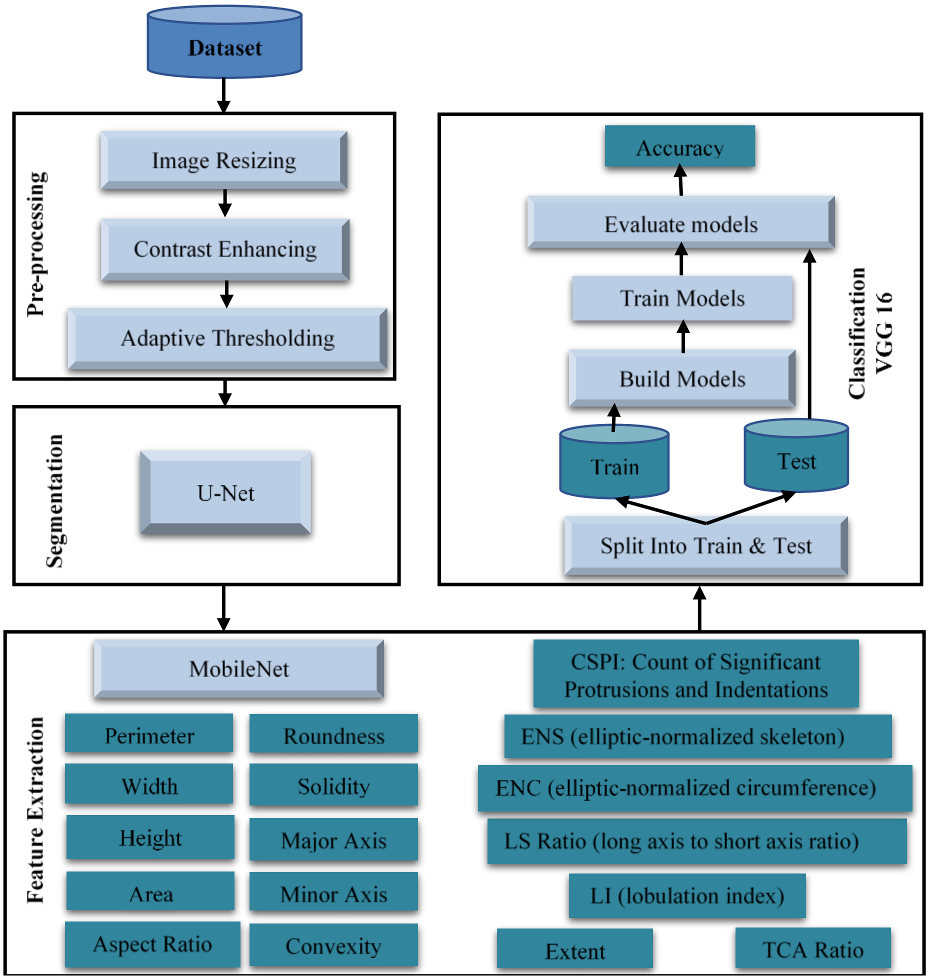

Figure 1. Proposed architecture

3.1. Dataset

In 2018, data were collected at baseline, which includes BUS images of women aged 25 to 75. The dataset, is obtained from Baheya Hospital for early detection and treatment of women's cancer in Cairo, Egypt, is divided into three classes: normal, benign, and malignant images. The dataset comprises 780 images without a mask and 1583 images with a mask, with an average image size of 500×500 pixels. The images are in PNG format, Figure 2 shows samples of breast images dataset.

Figure 2. Samples of US breast images

3.2. Pre-processing

Data pre-processing and cleaning: collecting and pre-processing the dataset of breast cancer images to prepare it for training and testing. The work first converts the colour format of the X-ray image from blue, green, and red (BGR) to RGB and applies thresholding to create a binary image. Detecting cancer and evaluating the properties including the following steps: i) file path for the image, ii) load the image, iii) convert the colour format from BGR to RGB, iv) apply thresholding to create a binary image, v) detect contours in the binary image, and vi) display the image.

3.3. Segmentation

Image segmentation is a digital process that divides an image into multiple segments [24], transforming it into meaningful objects for analysis. It is commonly used in breast imaging and digital mammography for detecting breast contours and identifying pectoral muscles [25], [26]. The study presents two models for a breast cancer X-ray image dataset: a segmentation model and a classification model. The U-net model, a group of convolutional networks designed for segmenting objects in digital images [27], uses high-resolution lesion information from the shallow layer and missing spatial information during upsampling for improved segmentation outcomes [28].

The U-Net architecture, designed for medical data scarcity, efficiently utilizes smaller datasets in DL, ensuring speed and precision without compromising on accuracy [29]. The U-Net model, a fully convolutional network (FCN) used for biomedical image segmentation, consists of an encoder, bottleneck module, and decoder, offering a U-shaped architecture, contextual information incorporation, rapid training speed, and efficient data utilization [30]. The U-Net architecture is unique due to its unique structure, consisting of a contracting path and an expansive path. The contracting path consists of encoder layers, capturing contextual information and reducing input spatial resolution, while the expansive path decodes encoded data [31]. U-Net uses a contracting path to identify features in images, convolutional operations to increase depth and spatial resolution, expansive path to decode encoded data while retaining input spatial resolution, and skip connections for better feature location [32].

The segmentation model is a U-Net model, which is a kind of CNN designed for image segmentation tasks. The model is trained on a dataset of X-ray images and their corresponding masks of tumor contours. The images are pre-processed and passed through the network, which outputs a predicted mask for each image. The model is then trained using the Adam optimizer and binary cross-entropy loss function. The model's performance is visualized using a line chart.

3.4. Feature extraction

Feature extraction is a process that reduces the dimensionality of raw data into manageable groups, reducing the volume of processing required while still accurately describing the original data set, especially in large datasets with numerous variables [33]. Feature extraction is a key component in mammogram classification, identifying and classifying abnormalities based on texture, statistical properties, spatial domain, fractal domain, and wavelet bases [34]. Implementing feature extraction techniques such as MobileNet, inception V3 and other technique to extract relevant features from the breast cancer images. This work also includes feature extraction for tumor contours. It then finds the contours in the binary image and draws them on the X-ray image. MobileNet is a low-cost, efficient CNN used for mobile vision tasks like object detection, fine-grained classification, face attributes, and localization [35]. MobileNets utilize depthwise separable convolutions to minimize computation in early layers, while flattened networks use fully factorized convolutions to demonstrate the potential of highly factorized networks [36].

The MobileNet model utilizes depthwise separable convolutions, which are a type of factorized convolutions that decompose a standard convolution into a depthwise convolution and a 1×1 convolution known as a pointwise convolution. In MobileNets, the depthwise convolution applies a single filter to each input channel, while the pointwise convolution combines the outputs of the depthwise convolution using a 1×1 convolution. Unlike a standard convolution, which filters and combines inputs into new outputs in a single step, the depthwise separable convolution divides this process into two separate layers for filtering and combining. This factorization significantly reduces computation and model size [37], [38].

The area, perimeter, height, width, count of significant protrusions and indentations (CSPI), aspect ratio, lobulation index (LI), elliptic-normalized skeleton (ENS), elliptic-normalized circumference (ENC), long axis to short axis (LS) ratio, convexity, extent, and tumor area to circle area (TCA) ratio, features of the contour are calculated and displayed and also fits an ellipse around the minimum area rectangle enclosing the largest contour and calculates the major and minor axis of the ellipse, roundness, and solidity [39], [40]. The features are:

a. Perimeter: the perimeter function measures the length of the tumor's boundary, which tends to be irregular in malignant tumors. A higher perimeter value is indicative of a higher probability of malignancy.
b. Height: bounding rectangle height (BRH), the height of the smallest rectangular area that contains the region of interest (ROI).
c. Width: bounding rectangle width (BRW), the width of the smallest rectangle that surrounds the ROI.

d. Area: the area feature represents the size of a breast tumor, with malignant tumors often exhibiting a larger area in comparison to benign tumors.
e. CSPI: the CSPI feature can be used to measure the extent of irregularity in the boundary.

The k-curve angle of a point, p_i, can be calculated using p_i, p_{i+k}, and p_{i-k}, where k is any number. P_i is smooth if θ_i is ≤ 40°, and convex or concave if θ_i is > 40°. If no concave points exist between convex and concave points, the convex point with the smallest k-curve angle is removed.

Figure 3 explains number of substantial protuberances and depressions, provides a demonstration of convex and concave points present in a tumor contour, followed by the definition of CSPI:

$$CSPI = 2 \times n \tag{1}$$

Where n represents the count of concave points. Malignant lesions typically exhibit a jagged boundary, resulting in a higher CSPI for malignant tumors. Figure 3 shows the concave and convex points for breast cancer. Malignant breast cancer contains convex points (triangle) and concave points (circle) as shown in Figure 3(a), while benign breast cancer contains convex points only (triangle) as shown in Figure 3(b).

Original cancer image | Mask of cancer image | Original image with mask, illustration of convex points (triangle) and concave points (circle) within the mask of a malignant breast cancer

(a)

Original cancer image (benign) | Mask of cancer image | Original image with mask, illustration of convex points only (triangle) because the benign tumor not contain concave points, it is most likely regular or semi-regular

(b)

Figure 3. The concave and convex points for breast cancer; (a) malignant breast cancer contains convex points (triangle) and concave points (circle) and (b) benign breast cancer contains convex points only (triangle)

f. LI: the lobe region bounded by a lesion contour and a line joined by any two neighboring concave points may be produced, in accordance with the definition for a concave point from the CSPI.

If the sizes of the biggest and smallest lobe areas are represented by A_{max} and A_{min}, and the average size of all lobe regions is represented by average, then LI may be defined as (2):

$$LI = \frac{(A_{max} - A_{min})}{A_{average}} \tag{2}$$

A malignant tumor often has a greater LI than a benign tumor.
g. ENS: the skeleton of a tumor region, S is intricate and intricate, with ENS representing the total points in S. Malignant tumors produce significant ENS and have twisted borders, as depicted in Figure 4.

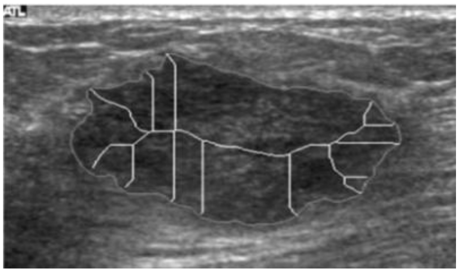

Figure 4. An illustration of a malignant breast tumor's skeleton (interior lines)

h. Aspect ratio: this is the length ratio between the width and depth of a tumor. A tumor has a higher chance of being malignant if its depth is bigger than its breadth and its aspect ratio is more than 1.

$$From\ factor = \frac{4\pi \times \text{Area}}{\text{Perimeter}^{2}} \tag{3}$$

The tumor is almost spherical when the form factor is approaching 1.

i. Roundness: the roundness formula measures how close a shape is to being circular. A roundness value near 1 indicates a nearly perfect circle, while values less than 1 suggest the shape is more irregular. It is commonly used in fields like geometry and engineering to assess circularity.

$$Roundness = \frac{(4 \times \text{Area})}{(\pi \times \text{Max Diameter}^{2})} \tag{4}$$

Where max diameter is the main axis length from the tumor's corresponding ellipse.

j. Solidity: it is near to 0, indicating that the tumor is malignant, and convex size is the size of the convex hull of a tumor.

$$Solidity = \frac{\text{Area}}{(\text{Convex\_Area})} \tag{5}$$

k. Major axis (MaA): the principal axis of the ellipse that fits the ROI the best.
l. Minor axis (MiA): the secondary axis of the ellipse that best fits the ROI.
m. ENC: the second-order moment can determine the inclination angle of each tumor in the x-y coordinate plane, allowing for the creation of an identical ellipse with the same area, center, and angle. The ENC may be defined as (6):

$$ENC = \frac{(Equivalent\ Ellipse\ Perimeter)}{(Perimeter)} \tag{6}$$

A smooth tumor border indicates a high probability of benignity when the ENC value of a suspected breast tumor is around 1.

n. LS ratio: the length ratio of the main long axis and minor short axis of the equivalent ellipse described in the ENC feature is known as the long axis to short axis ratio.
o. Convexity: it measures how closely a shape resembles its convex hull, calculated as the ratio of the convex perimeter to the actual perimeter. It ranges from 0 to 1, with convex shapes having a convexity of 1 and concave shapes having values less than 1. This metric is useful in shape analysis and image processing.

$$Convexity = \frac{Convex\ Perimeter}{Perimeter} \tag{7}$$

where the convex hull of a tumor's perimeter is known as its convex perimeter.

p. Extent: it measures how efficiently a shape fills its bounding rectangle, calculated as the ratio of the shape's area to the bounding box's area. It ranges from 0 to 1, with perfectly aligned rectangles having an extent of 1, while irregular shapes have lower values. This metric is useful in image processing and shape analysis.

$$Extent = \frac{Area}{Bounding\ Rectangle} \tag{8}$$

where the smallest rectangle that contains the tumor is called the bounding rectangle.

q. Tumor area to convex area ratio, or TCA ratio, is expressed as (9):

$$TCA\ Ratio = \frac{Area}{Convex\ Area} \tag{9}$$

3.5. Classification model

The classification model uses utilizing transfer learning with a VGG16 model that has been pre-trained model. The pre-trained layers are frozen, and a new classification model is added on top. Dividing the data into an 80% training set and a 20% validation set.

3.5.1. Training and testing deep learning models

Developing and testing machine learning models such as VGG, and CNNs to accurately classify breast cancer images. The VGG16 model is a 16-layer CNN architecture known for its exceptional performance in computer vision tasks. The first convolutional layer uses a kernel size of 11, while the second layer uses a kernel size of 5. Rather than relying on a multitude of hyper-parameters, VGG16 employs 3×3 filters and stride 1 in its convolution layers, with consistent use of same padding and 2×2 stride 2 maxpool layers throughout the architecture. The network concludes with two fully connected layers and a softmax for output. The "16" in VGG16 signifies the 16 layers with weights. This network is quite substantial, containing approximately 138 million parameters [41].

The new model consists of a flatten layer, a dense layer with 256 units, and a concluding dense layer featuring a sigmoid activation function. It has been trained on a dataset containing X-ray images classified as either benign or malignant. The model's performance is assessed and presented using a confusion matrix. After training, the actual and predicted masks were visualized for comparison. The classifier model was used to classify types of breast cancer, and the resulting classifications were visualized.

4. RESULTS AND DISCUSSION

4.1. Implementation

The authors used Kaggle to edit and run the code, which was built in Python version 3.11. Kaggle, founded in 2010 and acquired by Google in 2017, is an online platform for data science and machine learning competitions. It offers a community-driven environment for data scientists and enthusiasts to explore, analyze, and solve real-world data problems. Users can share code, notebooks, and insights related to data science projects on its cloud-based Jupyter Notebook environment called Kaggle Kernels, and using laptop properties processor Core i5, RAM 8 GB, Windows 10.

4.2. Evaluation

For evaluated the proposed system, a calculated number of criteria, parameters, and variables, these criteria are: confusion matrix is used including: true positive (TP), true negative (TN), false positive (FP), and false negative (FN).

$$Accuracy = \frac{TP+TN}{TP+TN+FP+FN} \tag{10}$$

$$Recall = \frac{TP}{TP+FN} \tag{11}$$

$$Precision = \frac{TP}{TP+FP} \tag{12}$$

$$Sensitivity = \frac{TP}{(TP+FP)} \tag{13}$$

$$Specificity = \frac{TN}{(TN+FP)} \tag{14}$$

$$F1 - Score\ or\ F - Measure = 2 \times \frac{(Recall \times Precision)}{(Recall + Precision)} \tag{15}$$

4.3. System walkthrough

Figure 5 shows the output of the pre-processing stage. First, the input image is provided; second, the bounding box of ROI is determined; and third, the output of ROI is zoomed. As shown in Figure 6(a) the real image, Figure 6(b) mask of tumor, and Figure 6(c) mirror of mask for breast cancer, can be easily calculated.

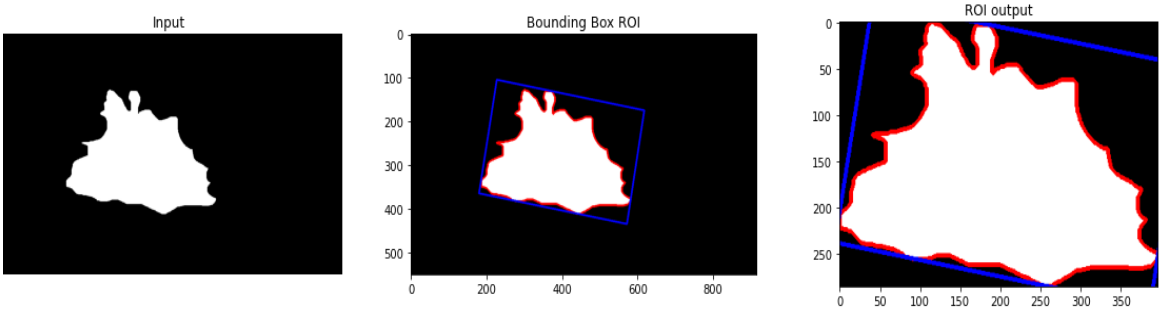

Figure 5. The output of the pre-processing phase

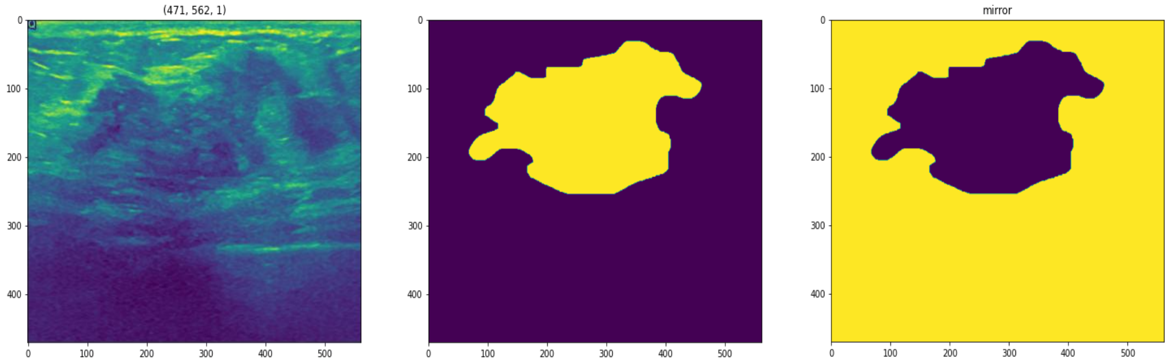

(a) (b) (c)

Figure 6. Mask of tumor; (a) main image, (b) mask of image, and (c) mirror of mask

The training parameters, we have 75 epochs, with batch size is 32 and learning rate 1e^{-2}. This batch size follows the recommendations of DL [42]. Table 2 shows the accuracy, loss, and area under the curve (AUC) of the training data. Accuracy measures the model's ability to predict correct labels or classes for training data, often used in classification tasks. Loss measures the discrepancy between predicted outputs and actual labels in training data, used to guide the model's learning process. AUC is a metric used in binary classification tasks to measure and evaluate the model's performance in terms of true positive rate (sensitivity) and false positive rate (1-specificity). A higher AUC indicates improved discrimination ability, with values falling between 0 and 1.

Table 2. The accuracy, loss, and AUC of the training

Accuracy	Loss	AUC
0.9868	0.0338	0.9978

Figure 7 shows explain the loss of train data. The training loss is calculated by averaging individual losses across the dataset, aiming to minimize it using optimization algorithms like gradient descent, thereby learning patterns that generalize well to unseen data.

Figure 8 shows the main image (Figure 8(a)), predicted mask (Figure 8(b)), and real mask (Figure 8(c)). A mask in computer vision is a binary image that indicates specific regions or objects of interest, used for object segmentation or image annotation. Real masks are manually annotated, representing the true segmentation of objects or regions, while predicted masks are generated by AI models or algorithms, attempting to automatically segment objects or regions in the main image. Table 3 shows the layer, parameters, and output shape of VGG classification.

Figure 7. The loss of train data

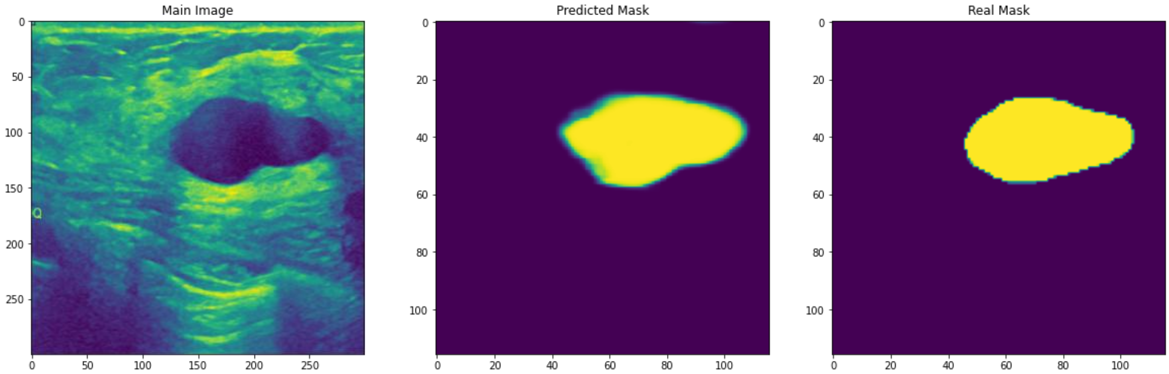

(a) (b) (c)

Figure 8. The predicted mask vs the real mask; (a) the main image, (b) the predicted mask, and (c) the real mask

Table 3. Layer, parameters, and output shape for VGG

Layer (type)	Output shape	Parameters
Flatten_1 (flatten)	(None, 25088)	0
Batch_normalization_ 1 (batch)	(None, 25088)	100352
Dense_2 (dense)	(None, 128)	3211392
Dense_3 (dense3)	(None, 3)	387
Total parameters: 3,312,131		
Trainable parameters: 3,261,955		
Non-trainable parameters: 50,176		

The testing parameters, we have 5 epochs, with batch size is 32. This batch size follows the recommendations of DL [40]. The learning rate is 0.001. Table 4 show the accuracy, validation accuracy, and loss for testing. We have 99.29% accuracy, with validation accuracy 90.48%. The loss is 0.0453, as shown in Table 4.

Table 4. The accuracy, validation accuracy, and loss for testing

Accuracy	Validation accuracy	Loss
0.9929	0.9048	0.0453

Figure 9 shows classification model performance. The loss started from 1.4 and is decreased to reach 0.0453. The accuracy started from beneath 0.8 and reached 0.9929. Figure 10 shows ability the proposed system to detect if an image belongs to which class, to be normal, malignant or benign. Figure 11 shows only those pictures that are predicted false. Rest of the pictures are predicted true. it’s just for clarification of the results.

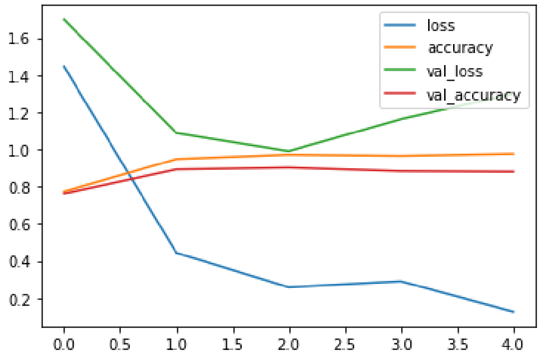

Figure 9. Classification model performance

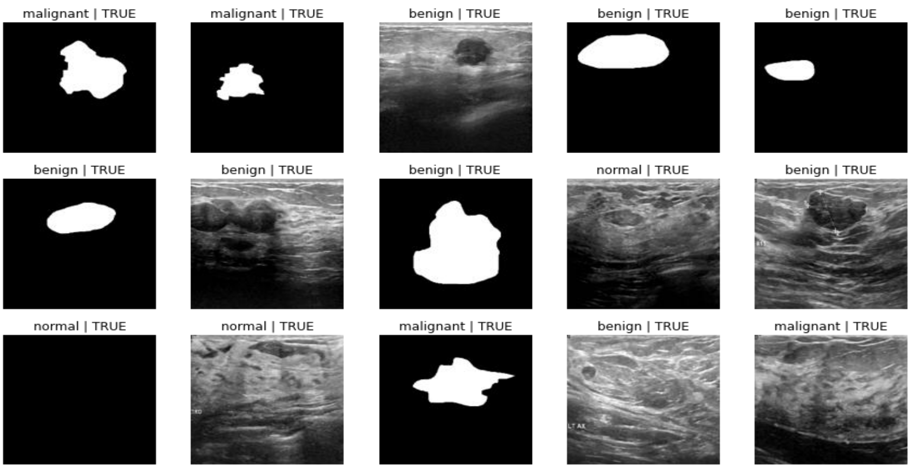

Figure 10. Predicting type of cancer normal, malignant, or benign

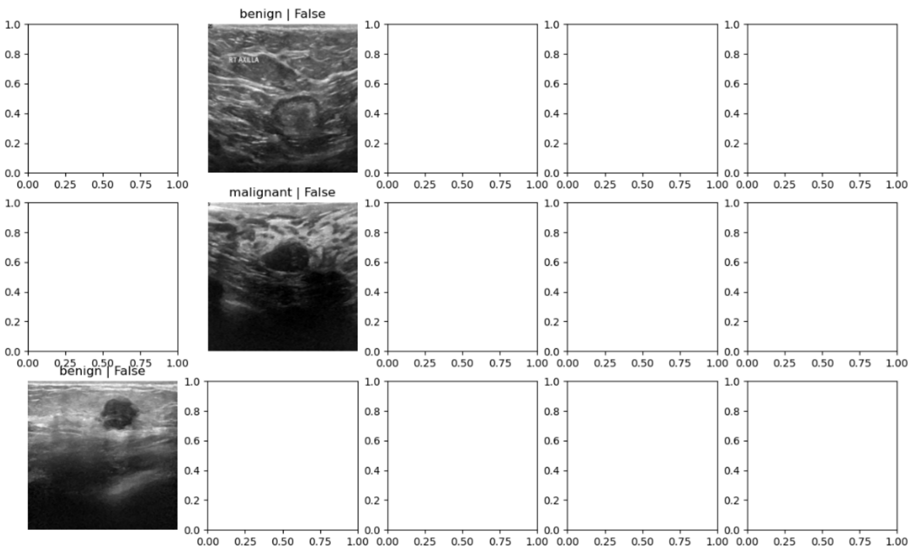

Figure 11. Those only pictures that are predicted false

Figure 12 shows the confusion matrix. It’s a tabular representation that shows the predicted and actual class labels for a set of data, providing a detailed analysis pertaining to the performance of a classification model, especially in scenarios with imbalanced classes. It consists of four key elements: TP, TN, FP, and FN. Table 5 lists the measurement of proposed system. The precision is 91.87%. sensitivity is 88.02% while specificity is 93.47%. The recall is 88.02% and the F1-score is 89.73%.

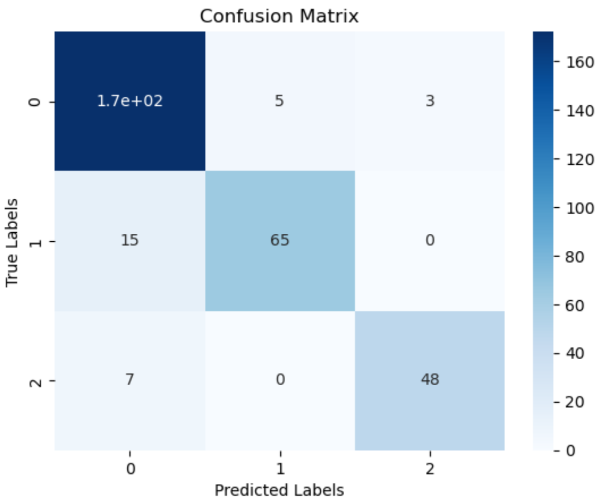

Figure 12. The confusion matrix

Table 5. The measurement of proposed system

Precision	Sensitivity	Specificity	Recall	F1-score (F-measure)
0.9187	0.8802	0.9347	0.8802	0.8973

4.4. Comparison and discussion

Table 6 shows the comparison. The proposed model exceeds the previous model in accuracy. It has 99.29% accuracy.

Table 6. Comparing proposed system with previous work

References	Accuracy (%)
[9]	92.95
[10]	73.0
[11]	94.62
[12]	94.23
[13]	97.9
[14]	89.73
[15]	90.41
[16]	95.48
[17]	91.5
[18]	97
[19]	97.17
[20]	95
[21]	90
[22]	88.67
[23]	89.8
Proposed system	**99.29**

In this work, the images were processed well before applying DL methods, in addition segmenting the images, isolating the tumor area and get the mask of tumor, and taking features from it. A large number of features were also extracted from the mask of tumor area, and then relying on these features to discover the tumor and determine its type in the classification stage. Furthermore, the predicted mask of tumor area and the predicted type of tumor based on the images. Many parameters were also calculated, such as accuracy, confusion matrix, sensitivity, specificity, and other. The proposed system outperformed previous work which worked on the same database, reaching 99.29% accuracy.

In recently work the image segmentation by using U-Net, was in study [9], the tumor regions were segmented from the BUS images using a supervised block-based region segmentation algorithm, with accuracy 92.95%. Pre-processing the image through three stages its: image resizing, contrast enhancing, and adaptive thresholding, while Cao *et al*. [10], remove the noisy labels during the training of breast tumor classification models, a successful technique known as the noise filter network with accuracy 73%, and Ilesanmi *et al*. [14], the images underwent resizing and were then enhanced using the contrast limited adaptive histogram equalization method and using the variant enhanced block the segmentation mask was generated through concatenated convolutions, with accuracy 89.73%, in study [16], the method applies fuzzy enhancement and bilateral filtering algorithms for the enhancement of original images, choose the optimal DL feature model, and train a network for classification that utilizes adaptive spatial feature fusion technology, with accuracy 95.48%, while study [21], work a standard for BUS image segmentation evaluation, for accurate annotations, and introduces a semi-automatic segmentation, with accuracy 90%.

In this paper provided extraction of a large number of features, while Moon *et al*. [11] provided a CAD system. This system combined various image content representations and employed ensemble techniques with different (CNN) architectures on US images, with accuracy 94.62%, and Zhang *et al*. [12] used (BI-RADS features) into task-oriented semi-supervised DL. This integration aimed to achieve precise diagnosis of US images, particularly when working with limited training data, with accuracy 94.23%.

This paper agreed with references [13] and [19], Byra *et al*. [13] used DL technique has been created for segmenting breast masses in US images, aiming to overcome the difficulty of automated segmentation caused by differences in breast mass size and image features, while Wang *et al*. [19], used a novel CNN with a coarse-to-fine feature fusion approach is suggested for breast image segmentation, with accuracy 97.9% and 97.17% respectively.

This paper carried out detection and classification of breast cancer-based US image, with the accuracy 99.29%, but Ayana *et al*. [18], introduced transfer learning methods for the classification and detection of breast images in US. The focus on pre-processing techniques, pre-training models, and CNN models, with accuracy 97%. In study [20], a BUViTNet, it's a method for BUS detection using ViTs instead of CNNs. The approach to classify BUS images. The performance of the algorithm with accuracy 95%, Kaplan *et al*. [22], the study proposes a BI-RADS a classifier model for categorizing US breast lesions using a novel multi-class US image, generate informative features for automated classification with accuracy 88.67%, and Feng *et al*. [23], to introduces an enhanced ViT. The model utilizes the output of the class token to distinguish between malignant and benign images. The output of each patch token is employed to determine if the patch overlaps with the tumor area with accuracy 89.8%.

4.5. Limitation of this work

Analyzing tumor images presents several challenges due to the variability in tumor shapes, particularly in malignant cases, which require precise masks for accurate segmentation. Extracting features solely from the tumor area is difficult, as isolating it from surrounding tissues is not always straightforward. Additionally, the large dimensions of medical images result in a high number of parameters, making the training and testing of DL models more complex and computationally demanding. These factors contribute to the difficulty of developing efficient and accurate tumor detection and classification systems.

5. CONCLUSION

This paper tried to present a proposed system for detecting the presence of breast cancer and classifying it by type based on US images of the tumor. The database contained benign, malignant and normal images that did not contain a tumor. The results showed that the proposed system was able to detect and classify well compared to previous work that worked on the same database, reaching accuracy of 99.29%. This paper worked on this type of tumors because it represents the second highest mortality rate in tumors around the world, especially in women according to international statistics. Early detection of the presence of this tumor leads to the possibility of survival, the effectiveness of treatment and cost reduction, as well as treatment before it is too late and the tumor spreads to the rest of the body, especially malignant tumors. The proposed system initially worked on processing medical images, removing the noise, then segmentation them and taking a mask of the tumor area, after which extracted the characteristics that rely on to detect and identify the type of tumor, and then the stage of classifying the type of tumor based on the characteristics that were extracted. The paper recommends that in future works, researchers shall be able to apply other techniques in DL, create a hybrid system of a combination of methods, techniques and compare them, and can also be applied to other databases.

FUNDING INFORMATION

Authors state no funding involved.

AUTHOR CONTRIBUTIONS STATEMENT

This journal uses the Contributor Roles Taxonomy (CRediT) to recognize individual author contributions, reduce authorship disputes, and facilitate collaboration.

Name of Author	C	M	So	Va	Fo	I	R	D	O	E	Vi	Su	P	Fu
Abdulqader Mohammed Khalaf		✓	✓		✓				✓		✓			
Mohammed Abdel Razek	✓					✓				✓		✓	✓	
Mohamed El-Dosuky		✓	✓		✓					✓	✓			
Ahmed Sobhi				✓		✓		✓		✓	✓			

C : **C**onceptualization
M : **M**ethodology
So : **So**ftware
Va : **Va**lidation
Fo : **Fo**rmal analysis
I : **I**nvestigation
R : **R**esources
D : **D**ata Curation
O : Writing - **O**riginal Draft
E : Writing - Review & **E**diting
Vi : **Vi**sualization
Su : **Su**pervision
P : **P**roject administration
Fu : **Fu**nding acquisition

CONFLICT OF INTEREST STATEMENT

Authors state no conflict of interest.

INFORMED CONSENT

We have obtained informed consent from all individuals included in this study.

DATA AVAILABILITY

Data is available at: https://www.kaggle.com/datasets/aryashah2k/breast-ultrasound-images-dataset.

REFERENCES

[1] G. N. Sharma, R. Dave, J. Sanadya, P. Sharma, and K. K. Sharma, "Various types and management of breast cancer: an overview," *Journal of advanced pharmaceutical technology & research*, vol. 1, no. 2, pp. 109–126, Apr. 2010.

[2] M. Kamińska, T. Ciszewski, K. Łopacka-Szatan, P. Miotła, and E. Starosławska, "Breast cancer risk factors," *Menopausal Review*, vol. 3, pp. 196–202, 2015, doi: 10.5114/pm.2015.54346.

[3] E. B. Ikhuoria and C. Bach, "Introduction to Breast Carcinogenesis – Symptoms, Risks factors, Treatment and Management," *European Journal of Engineering and Technology Research*, vol. 3, no. 7, pp. 58–66, Jul. 2018, doi: 10.24018/ejeng.2018.3.7.745.

[4] S. H. Jafari *et al.*, "Breast cancer diagnosis: Imaging techniques and biochemical markers," *Journal of Cellular Physiology*, vol. 233, no. 7, pp. 5200–5213, Jul. 2018, doi: 10.1002/jcp.26379.

[5] A. G. Waks and E. P. Winer, "Breast Cancer Treatment: A Review," *JAMA*, vol. 321, no. 3, pp. 288–300, 2019, doi: 10.1001/jama.2018.19323.

[6] R. Thackeray, S. H. Burton, C. Giraud-Carrier, S. Rollins, and C. R. Draper, "Using Twitter for breast cancer prevention: An analysis of breast cancer awareness month," *BMC Cancer*, vol. 13, no. 1, pp. 1-9, Dec. 2013, doi: 10.1186/1471-2407-13-508.

[7] T. Mahmood, J. Li, Y. Pei, F. Akhtar, A. Imran, and K. Ur Rehman, "A brief survey on breast cancer diagnostic with deep learning schemes using multi-image modalities," *IEEE Access*, vol. 8, pp. 165779–165809, 2020, doi: 10.1109/ACCESS.2020.3021343.

[8] T. G. Debelee, F. Schwenker, A. Ibenthal, and D. Yohannes, "Survey of deep learning in breast cancer image analysis," *Evolving Systems*, vol. 11, no. 1, pp. 143–163, Mar. 2020, doi: 10.1007/s12530-019-09297-2.

[9] W. X. Liao *et al.*, "Automatic Identification of Breast Ultrasound Image Based on Supervised Block-Based Region Segmentation Algorithm and Features Combination Migration Deep Learning Model," *IEEE Journal of Biomedical and Health Informatics*, vol. 24, no. 4, pp. 984–993, Apr. 2020, doi: 10.1109/JBHI.2019.2960821.

[10] Z. Cao, G. Yang, Q. Chen, X. Chen, and F. Lv, "Breast tumor classification through learning from noisy labeled ultrasound images," *Medical Physics*, vol. 47, no. 3, pp. 1048–1057, Mar. 2020, doi: 10.1002/mp.13966.

[11] W. K. Moon, Y. W. Lee, H. H. Ke, S. H. Lee, C. S. Huang, and R. F. Chang, "Computer-aided diagnosis of breast ultrasound images using ensemble learning from convolutional neural networks," *Computer Methods and Programs in Biomedicine*, vol. 190, pp. 1-12, Jul. 2020, doi: 10.1016/j.cmpb.2020.105361.

[12] E. Zhang, S. Seiler, M. Chen, W. Lu, and X. Gu, "BIRADS features-oriented semi-supervised deep learning for breast ultrasound computer-Aided diagnosis," *Physics in Medicine and Biology*, vol. 65, no. 12, pp. 1-16, Jun. 2020, doi: 10.1088/1361-6560/ab7e7d.

[13] M. Byra *et al.*, "Breast mass segmentation in ultrasound with selective kernel U-Net convolutional neural network," *Biomedical*

Signal Processing and Control, vol. 61, pp. 1-10, Aug. 2020, doi: 10.1016/j.bspc.2020.102027.
[14] A. E. Ilesanmi, U. Chaumrattanakul, and S. S. Makhanov, "A method for segmentation of tumors in breast ultrasound images using the variant enhanced deep learning," *Biocybernetics and Biomedical Engineering*, vol. 41, no. 2, pp. 802–818, Apr. 2021, doi: 10.1016/j.bbe.2021.05.007.
[15] T. Pang, J. H. D. Wong, W. L. Ng, and C. S. Chan, "Semi-supervised GAN-based Radiomics Model for Data Augmentation in Breast Ultrasound Mass Classification," *Computer Methods and Programs in Biomedicine*, vol. 203, pp. 1-8, May 2021, doi: 10.1016/j.cmpb.2021.106018.
[16] Z. Zhuang, Z. Yang, A. N. J. Raj, C. Wei, P. Jin, and S. Zhuang, "Breast ultrasound tumor image classification using image decomposition and fusion based on adaptive multi-model spatial feature fusion," *Computer Methods and Programs in Biomedicine*, vol. 208, pp. 1-9, Sep. 2021, doi: 10.1016/j.cmpb.2021.106221.
[17] M. Byra, "Breast mass classification with transfer learning based on scaling of deep representations," *Biomedical Signal Processing and Control*, vol. 69, pp. 1-8, Aug. 2021, doi: 10.1016/j.bspc.2021.102828.
[18] G. Ayana, K. Dese, and S. W. Choe, "Transfer learning in breast cancer diagnoses via ultrasound imaging," *Cancers*, vol. 13, no. 4, pp. 1–16, Feb. 2021, doi: 10.3390/cancers13040738.
[19] K. Wang, S. Liang, S. Zhong, Q. Feng, Z. Ning, and Y. Zhang, "Breast ultrasound image segmentation: A coarse-to-fine fusion convolutional neural network," *Medical Physics*, vol. 48, no. 8, pp. 4262–4278, Aug. 2021, doi: 10.1002/mp.15006.
[20] G. Ayana and S. W. Choe, "BUViTNet: Breast Ultrasound Detection via Vision Transformers," *Diagnostics*, vol. 12, no. 11, pp. 1-14, Nov. 2022, doi: 10.3390/diagnostics12112654.
[21] Y. Zhang *et al.*, "BUSIS: A Benchmark for Breast Ultrasound Image Segmentation," *Healthcare (Switzerland)*, vol. 10, no. 4, pp. 1-16, Apr. 2022, doi: 10.3390/healthcare10040729.
[22] E. Kaplan *et al.*, "Automated BI-RADS classification of lesions using pyramid triple deep feature generator technique on breast ultrasound images," *Medical Engineering and Physics*, vol. 108, Oct. 2022, doi: 10.1016/j.medengphy.2022.103895.
[23] H. Feng *et al.*, "Identifying Malignant Breast Ultrasound Images Using ViT-Patch," *Applied Sciences (Switzerland)*, vol. 13, no. 6, pp. 1-12, Mar. 2023, doi: 10.3390/app13063489.
[24] B. Chanda and D. D. Majumder, *Digital Image Processing and Analysis*. Prentice-Hall of India Pvt.Limited, 2011.
[25] R. Martí, A. Oliver, D. Raba, and J. Freixenet, "Breast skin-line segmentation using contour growing," in *Lecture Notes in Computer Science (including subseries Lecture Notes in Artificial Intelligence and Lecture Notes in Bioinformatics)*, Berlin, Heidelberg: Springer Berlin Heidelberg, 2007, pp. 564–571, doi: 10.1007/978-3-540-72849-8_71.
[26] D. Raba, A. Oliver, J. Martí, M. Peracaula, and J. Espunya, "Breast segmentation with pectoral muscle suppression on digital mammograms," in *Lecture Notes in Computer Science*, 2005, pp. 471–478, doi: 10.1007/11492542_58.
[27] H. Li, D. Chen, W. H. Nailon, M. E. Davies, and D. Laurenson, "Improved breast mass segmentation in mammograms with conditional residual U-net," in *Lecture Notes in Computer Science (including subseries Lecture Notes in Artificial Intelligence and Lecture Notes in Bioinformatics)*, 2018, pp. 81–89, doi: 10.1007/978-3-030-00946-5_9.
[28] S. Li, M. Dong, G. Du, and X. Mu, "Attention Dense-U-Net for Automatic Breast Mass Segmentation in Digital Mammogram," *IEEE Access*, vol. 7, pp. 59037–59047, 2019, doi: 10.1109/ACCESS.2019.2914873.
[29] A. O. Salau and S. Jain, "Feature Extraction: A Survey of the Types, Techniques, Applications," in *2019 International Conference on Signal Processing and Communication, ICSC 2019*, IEEE, Mar. 2019, pp. 158–164, doi: 10.1109/ICSC45622.2019.8938371.
[30] O. Ronneberger, P. Fischer, and T. Brox, "U-net: Convolutional networks for biomedical image segmentation," in *Lecture Notes in Computer Science (including subseries Lecture Notes in Artificial Intelligence and Lecture Notes in Bioinformatics)*, 2015, pp. 234–241, doi: 10.1007/978-3-319-24574-4_28.
[31] X. X. Yin, L. Sun, Y. Fu, R. Lu, and Y. Zhang, "U-Net-Based Medical Image Segmentation," *Journal of Healthcare Engineering*, vol. 2022, pp. 1–16, Apr. 2022, doi: 10.1155/2022/4189781.
[32] I. B. Ahmed, W. Ouarda, and C. B. Amar, "Hybrid UNET Model Segmentation for an Early Breast Cancer Detection Using Ultrasound Images," in *Lecture Notes in Computer Science (including subseries Lecture Notes in Artificial Intelligence and Lecture Notes in Bioinformatics)*, 2022, pp. 464–476, doi: 10.1007/978-3-031-16014-1_37.
[33] A. Baccouche, B. Garcia-Zapirain, C. Castillo Olea, and A. S. Elmaghraby, "Connected-UNets: a deep learning architecture for breast mass segmentation," *npj Breast Cancer*, vol. 7, no. 1, pp. 1-12, Dec. 2021, doi: 10.1038/s41523-021-00358-x.
[34] F. Moayedi, Z. Azirnifar, R. Boostani, and S. Katebi, "Contourlet-based mammography mass classification," in *Lecture Notes in Computer Science (including subseries Lecture Notes in Artificial Intelligence and Lecture Notes in Bioinformatics)*, Berlin, Heidelberg: Springer Berlin Heidelberg, 2007, pp. 923–944, doi: 10.1007/978-3-540-74260-9_82.
[35] W. Wang, Y. Li, T. Zou, X. Wang, J. You, and Y. Luo, "A novel image classification approach via dense-mobilenet models," *Mobile Information Systems*, vol. 2020, pp. 1–8, Jan. 2020, doi: 10.1155/2020/7602384.
[36] H. Hartatik and M. K. Anam, "Comparison of Convolutional Neural Network Architecture on Detection of Helmet Use by Humans," *Elinvo (Electronics, Informatics, and Vocational Education)*, vol. 8, no. 1, pp. 44–54, Jun. 2023, doi: 10.21831/elinvo.v8i1.52104.
[37] J. Hays and A. A. Efros, "IM2GPS: Estimating geographic information from a single image," in *26th IEEE Conference on Computer Vision and Pattern Recognition, CVPR*, IEEE, Jun. 2008, pp. 1–8, doi: 10.1109/CVPR.2008.4587784.
[38] A. G. Howard *et al.*, "MobileNets: Efficient Convolutional Neural Networks for Mobile Vision Applications," *arXiv*, Apr. 2017, doi: 10.48550/arXiv.1704.04861.
[39] Y. L. Huang, D. R. Chen, Y. R. Jiang, S. J. Kuo, H. K. Wu, and W. K. Moon, "Computer-aided diagnosis using morphological features for classifying breast lesions on ultrasound," *Ultrasound in Obstetrics and Gynecology*, vol. 32, no. 4, pp. 565–572, Sep. 2008, doi: 10.1002/uog.5205.
[40] Q. Zhang, T. Liu, T. Bao, Q. Li, and Y. Yang, "Development and External Validation of a Simple-To-Use Dynamic Nomogram for Predicting Breast Malignancy Based on Ultrasound Morphometric Features: A Retrospective Multicenter Study," *Frontiers in Oncology*, vol. 12, Apr. 2022, doi: 10.3389/fonc.2022.868164.
[41] S. Tammina, "Transfer learning using VGG-16 with Deep Convolutional Neural Network for Classifying Images," *International Journal of Scientific and Research Publications (IJSRP)*, vol. 9, no. 10, pp. 1-8, Oct. 2019, doi: 10.29322/ijsrp.9.10.2019.p9420.
[42] Y. Bengio, "Practical recommendations for gradient-based training of deep architectures," *Lecture Notes in Computer Science (including subseries Lecture Notes in Artificial Intelligence and Lecture Notes in Bioinformatics)*, vol. 7700 LECTURE NO, pp. 437–478, Jun. 2012, doi: 10.1007/978-3-642-35289-8_26.

BIOGRAPHIES OF AUTHORS

Abdulqader Mohammed Khalaf received the B.Sc. degrees in Computer Sciences from AL-Anbar University, in 2004. He received his M.Sc. degree in Human Computer Interaction (Brain Computer Interface) and Machine Learning from Mansoura University in 2016. Currently Ph.D. researcher of artificial intelligence (machine learning and deep learning) in Department of Mathematics and Computer Science, Faculty of Science, Al-Azhar University, Egypt. He can be contacted at email: mabdulqader135@gmail.com.

Mohammed Abdel Razek is Professor of Artificial Intelligence at Al-Azhar University, with a Ph.D. in Computer Science, obtained from the University of Montreal in 2004. Focused on AI techniques, his research spans diverse fields like healthcare, cybersecurity, e-learning, and IoT. He boasts an impressive publication record of over 85 papers in prestigious international journals and conferences. He is played a key role in establishing 17 e-learning centers at Egyptian universities during his tenure at the National E-learning Center and he is the founder of information and network unit at Al-Azhar University. Furthermore, he actively contributes to the establishment of ethical guidelines for AI usage by collaborating with the UNESCO-Egyptian committee. He can be contacted at email: abdelram@azhar.edu.eg.

Mohamed El-Dosuky received the B.S. and Master degrees in Computer Sciences from Mansoura University, in 2005 and 2008 respectively. He received his Ph.D. degree in Artificial Intelligence from Mansoura University in 2013. From 2013 to 2017, he managed to have a B.A. in Applied Sociology from Cairo University. He is the author of 5 books, and more than 90 articles. He is a member of ACM and IAENG. He is an Associate Professor at Department of Computer Science, Arab East Colleges, Saudi Arabia; and Department of Computer Science, Faculty of Computers and Information, Mansoura University, Egypt. His research interests include meta-heuristics optimization, quantum computing, blockchains, cybersecurity, and data science. He can be contacted at email: maldosuky@arabeast.edu.sa.

Ahmed Sobhi received his B.Sc. degree in Mathematics and Computer Science from Department of Mathematics, Faculty of Science, Al-Azhar University, Egypt in 2002. The M.Sc. degree in Computer Science from Faculty of Science, Minufiya University, Egypt in 2010. He obtained his Ph.D. in Computer Science from Department of Mathematics, Faculty of Science, Al-Azhar University, Egypt in 2017. He is a faculty member at Faculty of Science, Al-Azhar University since 2012. His research includes IoT, cloud computing, deep learning, and data science. He can be contacted at email: sobhi205@azhar.edu.eg.